Heat conduction in a rock mass with an annular hot water store

G. Rehbinder* and L. Reichel†

Vast subterranean caverns may be used for hot water storage in district heating schemes; such caverns can be annular, with a central pillar. This paper considers the quasi-steady solution of the heat conduction equation for this geometry with periodic temperature variations

Keywords: *heat storage, conduction, mathematical models*

Research into seasonal heat storage is attracting great interest in Sweden today. Surplus heat from industry or solar heat can be stored advantageously in large water-filled rock caverns (100 000–500 000 m^3). Relative heat losses are small if the volume is great and construction costs for rock caverns are relatively small.

If the total volume of the cavern is large, it may be necessary, for construction reasons, to build several separate caverns or an annular cavern with a 'pillar' left at its centre. The latter concept was used for the Lyckebo hot water store outside the city of Uppsala, Sweden, where an area including 550 apartments, shops, public buildings, schools etc, will be heated during the winter using the water heated during the summer by solar collectors. The shape and dimensions of the store are shown in Fig 1.

The design of an annular hot water store has several interesting facets. One is that the pillar contributes to storage performance in a more pronounced way than the rest of the surrounding rock. It is, therefore, of interest to study the interaction between the heat stored in the water in the cavern, the heat stored in the pillar, and the heat stored in the surrounding rock.

The operation of a seasonal hot water store implies that the temperature varies between two limits well above the undisturbed ground temperature. The consequence of this is that the net heat loss is proportional to the difference between the average temperature of the water in the store and the temperature of the undisturbed ground, to the length scale of the cavern and to the heat conduction coefficient of the rock. Initially when the heating of the water starts, the rock will consume considerable heat and the net losses will be great.

Theoretically, quasi-steady state will be reached after infinite time but, from a practical point of view, one can say that 3 years after the moment when the heating starts the 'pillar' has almost the average temperature of the water. Considering the heat flux to infinity, one can say that it takes 5 years for the average heat loss to decrease to twice the steady value. These simple estimations are easily found from the solutions given by Carslaw and Jaeger[1].

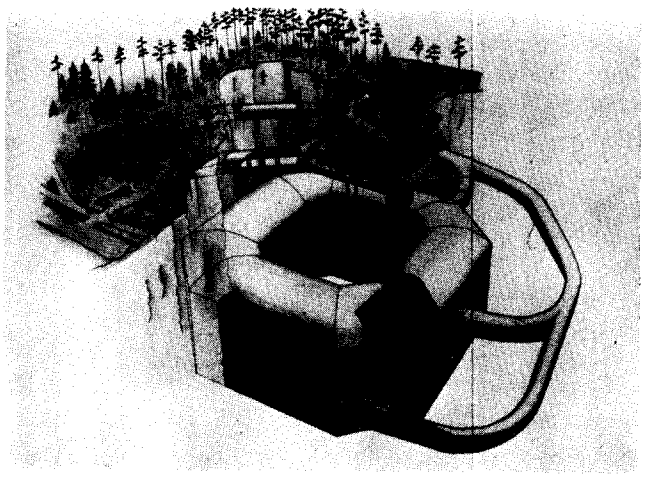

Fig 1 Hot water storage system at Lyckebo, Sweden

The aim of this paper is to study theoretically the quasi-steady solution of the heat conduction equation for periodic temperature variations. In the general case this is identical to an exterior Helmholtz problem. Such a theoretical investigation makes it possible to calculate the heat flow between the rock and the water in the cavern. This is of great interest since the heat flow always counteracts the loading and unloading of the store. It also makes it possible to calculate the temperature in the pillar, especially its damping and phase lag to the temperature in the storage. This latter study is most interesting since the temperature induces stresses and deformations in the pillar and it is not *a priori* evident that the pillar carries a pressure load thus supporting the over-burden.

The following analysis is based upon a number of simplifications and assumptions. We assume that the convection of heat with the ground water can be neglected. We also assume that the density and heat capacity of the rock are constants and that the heat conduction coefficient is isotropic and constant. Finally we assume that the cavern is a torus with cylindrical symmetry. The cavern is assumed to be located well below the ground, implying that the presence of a free ground surface can be

* Swedish Rock Mechanics Research Foundation, Stockholm, Sweden
† Mathematics Research Center, University of Wisconsin, Madison, Wisconsin, USA
Received 18 February 1983 and accepted for publication on 5 December 1983

neglected. The first assumptions, dealing with the rock properties, are reasonable; for economic reasons the cavern has been located in very good quality rock. The shape of the cavern is not perfectly symmetrical but the deviation is small. The last assumption, that the ground surface has no influence, is the most questionable since the distance between the top and bottom of the cavern is equal to the distance between the top of the cavern and the ground surface. This difficulty can of course be avoided by the use of the method of image, a calculation planned but not yet performed.

Non-dimensional equations

Consider a region exterior to a torus Ω symmetric with respect to the z-axis, with the boundary $\partial\Omega$. Let the inner radius of $\partial\Omega$ be the characteristic length a of the problem (Fig 2). At $\partial\Omega$ the temperature T is prescribed $T_0\Phi(t,r)$ where the constant T_0 is the characteristic temperature of the problem, and $\Phi(t,r)$ is a given function of $[0,\infty)\times\partial\Omega$. The temperature is assumed to vanish at infinity. The initial temperature is zero. The region consists of a rock whose heat conduction is λ, heat capacity c and density ρ. These parameters can be combined giving the diffusivity $\kappa=\lambda/\rho c$. Thus with cylindrical coordinates:

$$\frac{\partial T}{\partial t}=\kappa\left(\frac{\partial^2 T}{\partial r^2}+\frac{1}{r}\frac{\partial T}{\partial r}+\frac{\partial^2 T}{\partial z^2}\right) \quad \text{in } \boldsymbol{R}^3\backslash\Omega \tag{1}$$

$$T(r,z,t)=T_0\Phi(t,r) \quad \text{on } \partial\Omega \quad t\geqslant 0 \tag{2}$$

$$T(r,z,t)=0 \quad r^2+z^2\to\infty \quad t>0 \tag{3}$$

$$T(r,z,t)=0 \quad \text{in } \boldsymbol{R}^3\backslash\Omega \quad t<0 \tag{4}$$

A general solution is not easily found. It has recently been shown by Brander and Rehbinder[2] that the solution can be expressed with the T-matrix representation used in scattering theory. As mentioned in the introduction our aim is to solve the limiting problem $\phi(t,r)=\exp(i\omega t)$ when $t\to\infty$. Introducing the following variables:

$$u=Te^{-i\omega t}/T_0 \tag{5}$$

$$\xi=r/a \tag{6}$$

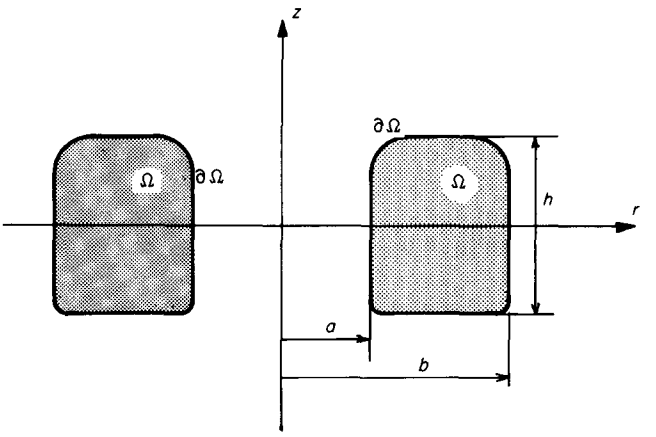

Fig 2 The torus Ω

$$\zeta=z/a \tag{7}$$

$$\tau=\kappa t/a^2 \tag{8}$$

$$\hat{b}=b/a \tag{9}$$

$$\hat{h}=h/a \tag{10}$$

$$\hat{\omega}=\omega a^2/\kappa \tag{11}$$

$$k=e^{3\pi i/4}\hat{\omega}^{1/2} \tag{12}$$

the heat conduction problem above is then reduced to a boundary value problem for the Helmholtz equation. The parameters a, b and h can be varied to study their effect on u.

Numerical approximation by particular solutions

In accordance with the discussion above, we will solve the Helmholtz problem in cylindrical coordinates:

$$\frac{\partial^2 u}{\partial\xi}+\frac{1}{\xi}\frac{\partial u}{\partial\xi}+\frac{\partial^2 u}{\partial\zeta}+k^2u=0 \quad \text{in } \boldsymbol{R}^3\backslash\Omega \tag{13}$$

$$u=1 \quad \text{on } \partial\Omega \tag{14}$$

$$\lim_{R\to\infty} R\left(\frac{\partial u}{\partial R}-iku\right)=0 \qquad R=\sqrt{\xi^2+\zeta^2} \tag{15}$$

Notation

a_{rj}	Multipole coefficients
a	Inner radius of the torus
b	Outer radius of the torus
$\hat{b}$	Dimensionless outer radius of the torus, b/a
c	Heat capacity of the rock
$G_j(z)$	Greens' function
h	Height of the torus
$\hat{h}$	Dimensionless height of the torus, h/a
$H_j(z)$	Harmonic auxiliary function
$j,l,m,$ n,p,q	Auxiliary parameters (natural numbers)
K_ν, I_ν	Modified Bessel functions
M_ν, N_ν	Amplitudes of Kelvin functions
r	Radial coordinate
$\bar{r}'$	(ξ',θ',ζ')
$\bar{r}$	(ξ,θ,ζ)
s'	Arclength along the circle γ_j
T	Temperature
T_0	Reference temperature
t	Time
u	Dimensionless amplitude of the temperature
w_j	Auxiliary coordinate
z	Axial coordinate
ξ	Dimensionless radial coordinate, r/a
θ	Azimuthal coordinate
ζ	Dimensionless axial coordinate, z/a
ξ',θ',ζ'	Integration variables
τ	Dimensionless time, $t\kappa/a^2$
λ	Heat conduction coefficient of the rock
ρ	Density of the rock
κ	Heat diffusivity of the rock, $\lambda/\rho c$
ω	Circular frequency
$\hat{\omega}$	Dimensionless circular frequency, $\omega a^2/\kappa$
θ_ν, ϕ_ν	Phase of Kelvin function
γ_j	Circular curve within the torus
Γ	Cross section curve of the torus
Ω	Region occupied by the torus
Φ	Dimensionless temperature in the torus

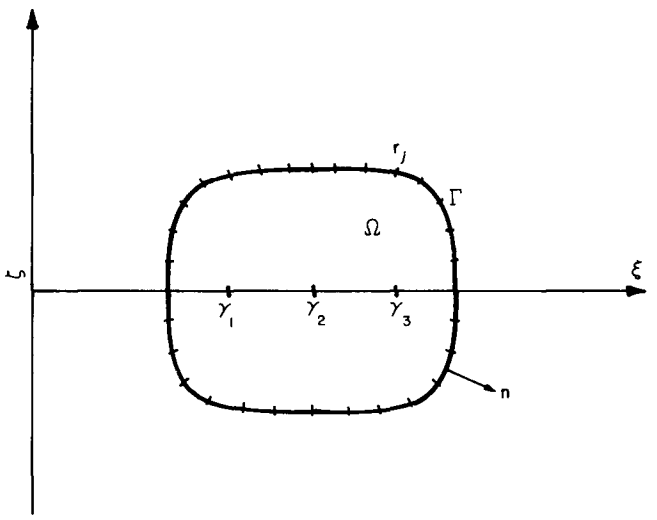

Fig 3 Torus Ω showing the location of the collocation points and the circles γ_j

Eq (15) is the Sommerfeld radiation condition, ensuring the unique solvability of Eqs (13)–(15).

We will seek the solution in the form of a linear combination of particular solutions, which satisfy Eqs (13) and (15). The linear combination is to be chosen so that Eq (14) is approximately satisfied. By using cylindrically symmetric particular solutions, we will see that the cylindrically symmetric three-dimensional problem on an infinite domain is reduced to a one-dimensional approximation problem on a curve of finite length. We will also indicate how fully three-dimensional problems can be treated by this approach. Compared to integral equation methods, our approach has the advantage that no singular integrals have to be computed. This simplifies programming.

Our numerical method requires some decisions. We must:

1. Choose a subspace of particular solutions and select a basis for this subspace;
2. Choose a finite set of points on the boundary, the collocation points where we require the boundary conditions to be satisfied.

In this section, we describe the particular solutions chosen and in the next section we discuss the selection of collocation points.

There are still some open theoretical questions under investigation on the choices above. In the selections described we have been guided by experience gained from solving two-dimensional problems (see 'Section rationale' below).

Let γ_j, $j=1(1)n$, be circles in the interior of Ω and symmetric with respect to the ζ-axis (Fig 3). Let $\bar{r}$ and $\bar{r}'$ be vectors with cylindrical coordinates $\bar{r}=(\xi,\theta,\zeta)$ and $\bar{r}'=(\xi',\theta',\zeta')$. Then for $\bar{r}\in(\boldsymbol{R}^3\backslash\Omega)\cup\partial\Omega$, $J=1(1)n$;

$$u_{lj}(\bar{r})=\int_{\gamma_j}\frac{\partial^{l-1}}{\partial r'^{l-1}}\left(\frac{e^{ik|\bar{r}-\bar{r}'|}}{|\bar{r}-\bar{r}'|}\right)ds' \qquad l=1,2,3\ldots \tag{16}$$

are particular solutions of Eq (13), independent of θ and satisfying Eq (15). We are to determine the coefficients a_{lj} in:

$$\tilde{u}(\bar{r})=\sum_{l=1}^{m}\sum_{j=1}^{n}a_{lj}u_{lj}(\bar{r}) \tag{17}$$

so that the boundary condition (Eq (14)) is approximately satisfied. Due to the cylindrical symmetry this is a one-dimensional approximation problem. Typical values for m and n used in the computation have been $4\leqslant m\leqslant 6$ and $4\leqslant n\leqslant 7$. Explicit expressions for some u_{lj} are given in the appendix. Note that the kernels are smooth and that the integrals can be computed conveniently by the trapezoidal rule. The following remarks provide some background to the selection of m, n and γ_j.

Selection rationale

Our motivation for selecting n, the number of circles γ_j, greater than 1 is that for oblong cross sections this gives considerably higher accuracy than computation with $n=1$. On the other hand if we seek a linear combination of u_{1j}, $j=1(1)n$, $m=1$, where the circles γ_j come close, the resulting linear system is severely ill-conditioned. The numerical condition improves if we replace close circles by one circle on which we allow multipoles, ie we reduce n and increase m. Since neither the placement of circles nor the choice of m is critical for the computation, these guidelines suffice to achieve high enough accuracy for many applications. An estimate of the error in the computed solution of Eqs (13)–(15) can be obtained by computing the deviation of the determined linear combination (Eq (16)) from 1 on $\partial\Omega$. Also, when the Laplace equation is to be solved in exterior regions, choices analogous to those of n, m and γ_j have to be made. For two-dimensional problems for the Laplace equation, the influence of these selections on the rate of convergence and numerical conditioning has been analysed elsewhere[5].

Note also that, for problems with no cylindrical symmetry, the particular solutions u_{lj} are replaced by function:

$$\tilde{u}_{lj}(\bar{r})=\frac{\partial^{l-1}}{\partial r'^{l-1}}\left(\frac{e^{ik|\bar{r}-\bar{r}_j'|}}{|\bar{r}-\bar{r}_j'|}\right),$$
$$j=1(1)n,\quad l=1,2,3,\ldots \tag{18}$$

where $\bar{r}_j'$ are points distributed in the interior of Ω.

Least squares collocation

We introduce the curve Γ defined as the intersection between $\partial\Omega$ and the half plane $\theta=0$. We also allocate a number, ranging between $2mn$ and $3mn$, of collocation points $\bar{r}_j$ on Γ and require $\tilde{u}(\bar{r})$ to satisfy the boundary condition (Eq (14)) at all $\bar{r}_j$ in the least-squares sense. The largest number of points was used in cases when the thickness of Ω was relatively small. That the system of linear equations is over constrained makes the computation less sensitive to the distribution of collocation points than if an $mn\times mn$ system were to be solved. Nevertheless, the allocation of collocation points is important and we will therefore describe the distribution principles. The allocation method is a simplified version of a strategy previously used for two-dimensional problems for the Laplace operator (discussed below). Putting monopoles of unit density over each circle γ_j yields the potential:

$$v(\bar{r})=\sum_{j=1}^{n}\int_{\gamma_j}\frac{1}{|\bar{r}-\bar{r}'|}ds' \tag{19}$$

Let $\bar{n}$ be the exterior unit normal to Γ in the plane $\theta=0$. Then $\partial v/\partial n<0$ and:

$$2\pi\int_\Gamma |\bar{r}|\frac{\partial v}{\partial n}ds=-4\pi\sum_{j=1}^{n}2\pi(\text{radius of }\gamma_j) \tag{20}$$

Let:

$$s_d(\bar{r})=\frac{-|\bar{r}|\dfrac{\partial v(\bar{r})}{\partial n}}{4\pi\displaystyle\sum_{j=1}^{n}\text{radius of }\gamma_j} \tag{21}$$

be the density function for the collocation points on Γ. To compute $s_d(\bar{r})$, we approximate $\partial v/\partial n$ by a trigonometric polynomial, which we integrate and normalize to obtain the distribution function $\tilde{s}_d(\bar{r})$. Then p collocation points $\{\bar{r}_j\}_1^p$ are determined by solving the equations:

$$\tilde{s}_d(\bar{r}_j)=\frac{j-1}{p}\qquad j=1,2,3,\ldots,p \tag{22}$$

For fully three-dimensional problems Eq (19) is to be replaced by:

$$\tilde{v}(\bar{r})=\sum_{j=1}^{n}\frac{1}{|\bar{r}-\bar{r}_j|} \tag{23}$$

where the sum is over all distinct points $\bar{r}_j$. On $\partial\Omega$ one allocates collocation points so that if they were point charges of equal charge they would produce a potential in $\boldsymbol{R}^3\backslash\Omega$ which approximates the potential obtained from Eq (23). The accuracy requirement is not high.

To motivate Eqs (19)–(23) we conclude this section with an outline of the allocation of collocation points for two-dimensional problems for the Laplace equation. More details have been given elsewhere[4,5]. Let Ω_2 be an open bounded, simply connected region in the plane, which we identify with the complex plane $\mathbf{C}$. Let f be a continuous real-valued function on $\partial\Omega_2$ and consider the Dirichlet problem:

$$\begin{aligned}&\Delta u=0 && \text{in } \boldsymbol{C}\backslash\Omega_2\\ &u=f && \text{on } \partial\Omega_2\\ &u && \text{bounded at infinity}\end{aligned} \tag{24}$$

Let $\omega_j, j=1(1)n$, be distinct points in Ω_2. An approximate solution to Eq (23) is sought in the form:

$$u=a_0+\sum_{j=1}^{n}Re\left(\sum_{l=1}^{m}a_{lj}(z-w_j)^{-l}\right) \tag{25}$$

where $a_0\in\boldsymbol{R}$ and $a_{lj}\in\boldsymbol{C}$. To determine the coefficients one needs at least $2nm+1$ collocation points z_κ. To describe a suitable allocation of the z_κ we introduce Green's functions $G_j(z)$ for the Laplace operator on Ω_2 with a logarithmic singularity at $z=\omega_j$. The $G_j(z)$ are uniquely determined by:

$$G_j(z)=\frac{1}{2\pi}\ln\frac{1}{|z-w_j|}+H_j(z) \tag{26}$$

where $H_j(z)$ is harmonic in Ω_2 and:

$$H_j(z)=-\frac{1}{2\pi}\ln\frac{1}{|z-w_j|}$$

on $\partial\Omega_2$. Let $\partial/\partial n$ denote the normal derivative into Ω_2 and allocate $q\geqslant 2nm+1$ collocation points equidistantly with respect to the density function:

$$s(z)=\frac{1}{n}\sum_{j=1}^{n}\frac{\partial G_j}{\partial n}(z)\qquad z\in\partial\Omega_2, \tag{27}$$

ie require:

$$s(z_j)=\frac{j-1}{q}\qquad j=1(1)q. \tag{28}$$

This allocation has been studied elsewhere[4,5] and certain convergence results presented there. A density function that is simpler to compute than Eq (27) is obtained by neglecting the $H_j(a)$:s in Eq (26). The modified density function becomes:

$$s(z)=\frac{1}{2\pi n}\sum_{j=1}^{n}\frac{\partial}{\partial n}\ln\frac{1}{|z-w_j|}. \tag{29}$$

When using this density function more collocation points than unknowns should be used. For rotationally symmetric problems (Eq (21) is the analogue of Eq (29). For fully three-dimensional problems the analogue of Eq (24) is Eq (23).

Solutions for pure radial flow

If $\hat{h}\gg 1$, the solution of Eqs (13)–(15) in the vicinity of $\zeta=0$ is equal to the solutions for pure radial flow. These solutions can be found in Carslaw and Jaeger's textbook[1]. Thus:

$$u=\frac{K_0(k\xi)}{K_0(k\hat{b})}\qquad \xi\geqslant\hat{b}\quad |k|>0 \tag{30}$$

$$u=\frac{I_0(k\xi)}{I_0(k)}\qquad \xi\leqslant 1 \tag{31}$$

The modified Bessel functions K_v and I_v for a complex argument are most conveniently expressed[3] with the modulii M_v and N_v and phases θ_v and ϕ_v of Kelvin's functions. We can then write the solutions in simple form:

$$u(\xi)=\frac{N_0(\xi\sqrt{\hat{\omega}})}{N_0(\hat{b}\sqrt{\hat{\omega}})}e^{i(\phi_0(\xi\sqrt{\hat{\omega}})-\phi_0(\hat{b}\sqrt{\hat{\omega}}))}\qquad \xi\geqslant\hat{b} \tag{32}$$

$$u(\xi)=\frac{M_0(\xi\sqrt{\hat{\omega}})}{M_0(\sqrt{\hat{\omega}})}e^{i(\theta_0(\xi\sqrt{\hat{\omega}})-\theta_0(\sqrt{\hat{\omega}}))}\qquad \xi\leqslant 1 \tag{33}$$

The derivatives of these functions on $\partial\Omega$ are:

$$\left(\frac{\partial u}{\partial\xi}\right)_{\xi=\hat{b}}=\sqrt{\hat{\omega}}\frac{N_1(\hat{b}\sqrt{\hat{\omega}})}{N_0(\hat{b}\sqrt{\hat{\omega}})}e^{i(\phi_1(\hat{b}\sqrt{\hat{\omega}})-\phi_0(\hat{b}\sqrt{\hat{\omega}})+\pi/4)} \tag{34}$$

$$\left(\frac{\partial u}{\partial\xi}\right)_{\xi=1}=\sqrt{\hat{\omega}}\frac{M_1(\sqrt{\hat{\omega}})}{M_0(\sqrt{\hat{\omega}})}e^{i(\theta_1(\sqrt{\hat{\omega}})-\theta_0(\sqrt{\hat{\omega}})+\pi/4)} \tag{35}$$

Generally $\boldsymbol{R}^3\backslash\Omega$ is doubly connected but in this case where $\hat{h}\to\infty$ the region $\boldsymbol{R}^3\backslash\Omega$ is split in two separate regions $\xi\leqslant 1$ and $\xi\geqslant\hat{b}$ which do not interact. The solutions given by Eqs (32) and (33) are shown graphically in Figs 4–8 together with the numerical solutions for $\hat{h}<\infty$.

The gradients at the inner and outer boundaries of Ω given by Eqs (34) and (35) make it possible to study the relation between the heat fluxes leaving and returning to Ω. Fig 9 shows the ratio between the heat flux q_{out} going outwards through $\xi=\hat{b}$ and the heat flux q_{in} going inwards through $\xi=1$. We can see that the flux is mainly

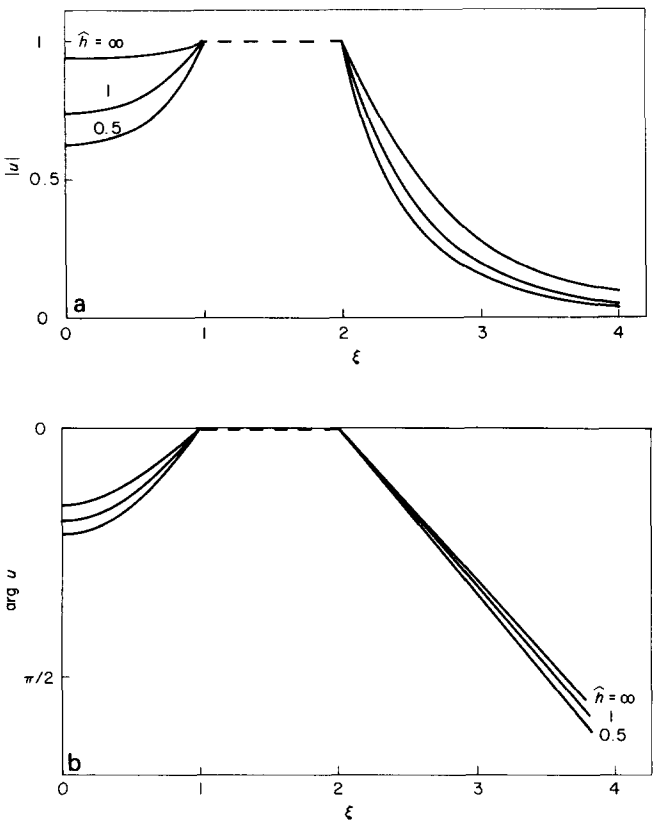

Fig 4 Absolute value and phase of the temperature in the symmetry plane $\zeta=0$; $\hat{\omega}=2$, $\hat{b}=2$

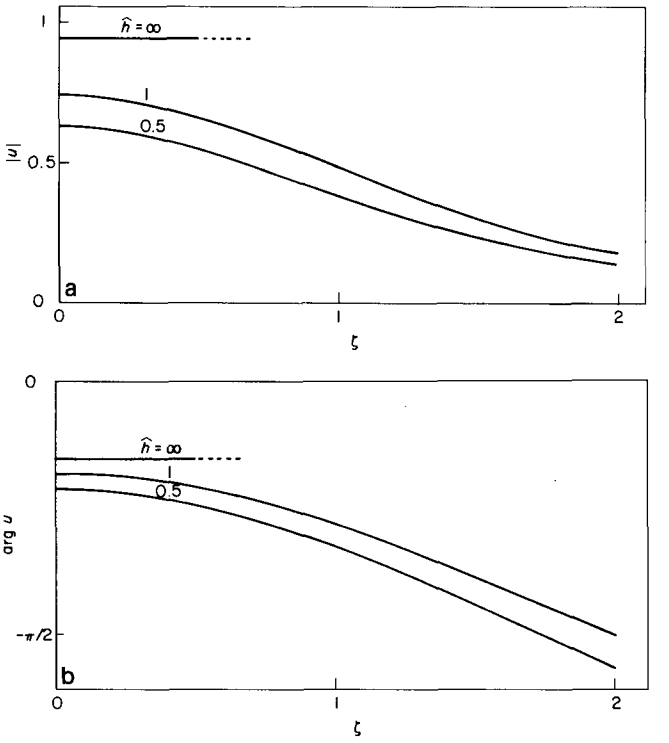

Fig 6 The absolute value and phase of the temperature on the symmetry line $\xi=0$; $\hat{\omega}=2$, $\hat{b}=2$

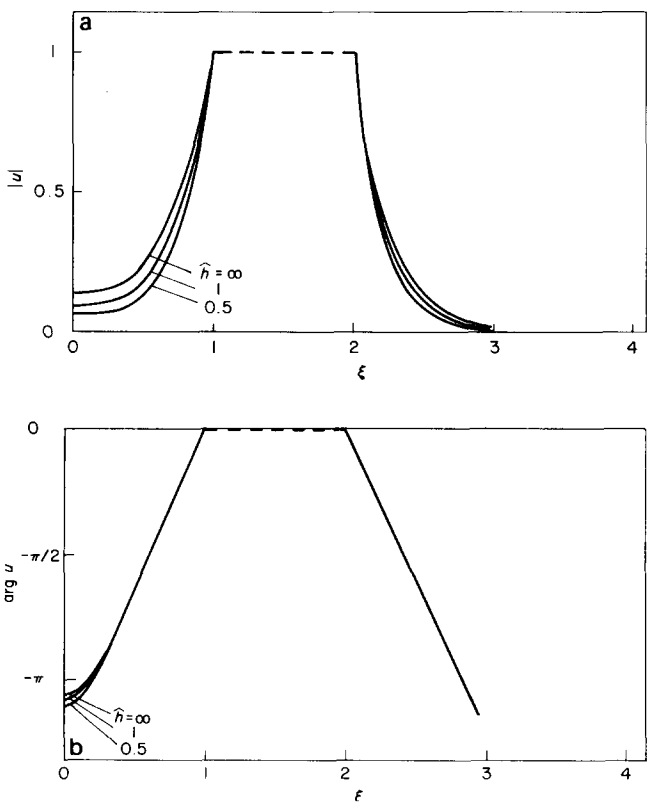

Fig 5 Absolute value and phase of the temperature in the symmetry plane $\zeta=0$; $\hat{\omega}=30$, $\hat{b}=2$

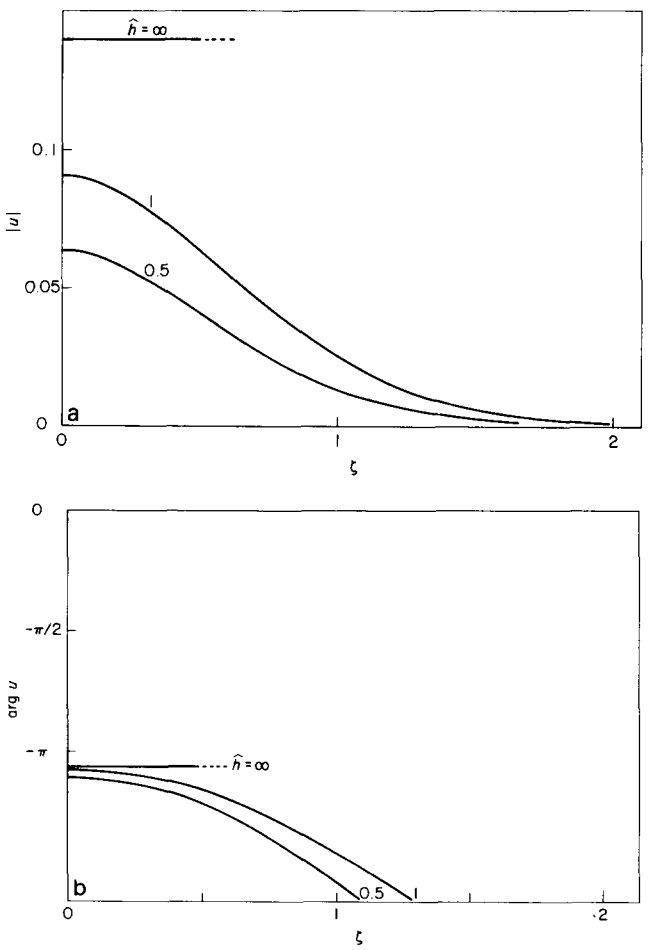

Fig 7 Absolute value and phase of the temperature on the symmetry line $\xi=0$; $\hat{\omega}=30$, $\hat{b}=2$

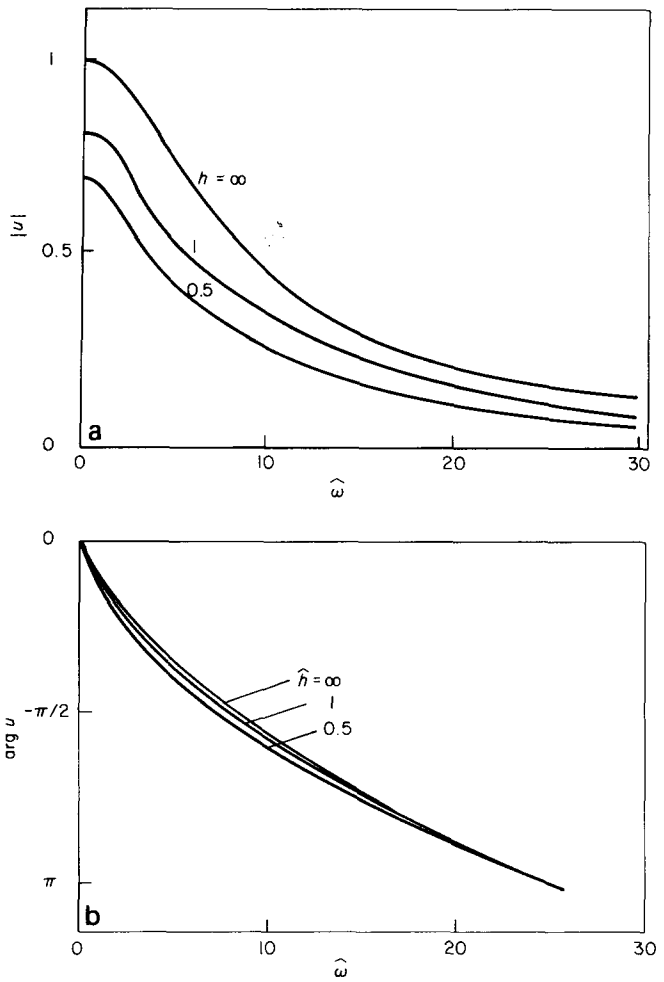

Fig 8 Absolute value and phase of the temperature in the symmetry point $\xi=\zeta=0$ as a function of the frequency; $\hat{b}=2$

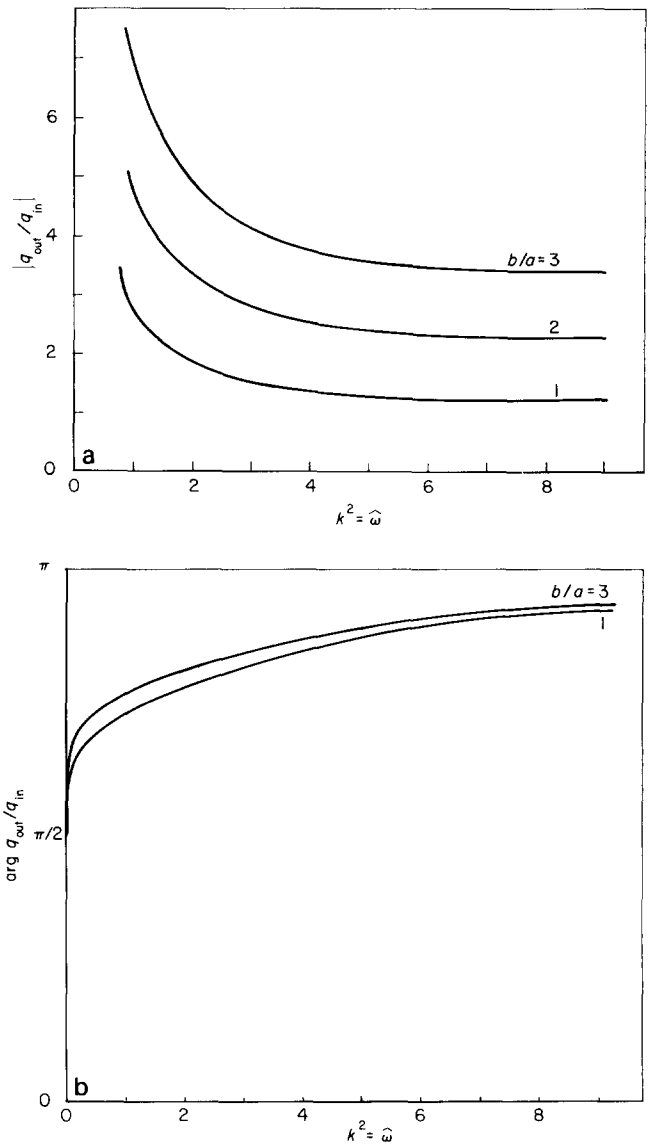

Fig 9 Absolute value and phase of the ratio between the heat fluxes through the boundaries $\xi=\hat{b}$ and $\xi=1$ as a function of the frequency; cylindrical flow

determined by the area of the heated surface. We also see that if the frequency is high the fluxes are shifted 180°.

Solution for a circular torus with a superelliptic cross-section

In a practical case, $\hat{h}=\mathcal{O}(1)$ and we wish to calculate u at certain points. The most interesting points are those where the solution can be compared with that of the previous section.

For the practical computation we have chosen Γ to be a superellipse such that:

$$\Gamma:\left(\frac{2\zeta}{\hat{h}}\right)^4+\left(\frac{2\xi-\hat{b}-1}{\hat{b}-1}\right)^4=1 \qquad (36)$$

Let $\gamma_j, j=1,2,3$ be circles in the plane $\zeta=0$ so that γ_j passes through $\xi=j+1$, $\theta=0, \pi/2$. Γ and γ_j are shown in Fig 3. The dashes on Γ mark the collocation points obtained from Eq (21). In our computation we have used the following values:

$\hat{b}=2$

$\hat{h}=0.5, 1$

$\hat{\omega}=0, 2, 5, 15, 30$

$0\leqslant\xi\leqslant 1 \qquad \xi\geqslant\hat{b} \qquad \zeta=0$

$0\leqslant\xi\leqslant 2 \qquad \xi=0$

We have thus calculated the function $u(\xi,\zeta;\hat{\omega},\hat{h},\hat{b})$ on the symmetry plane $\zeta=0$ and on the symmetry line $\xi=0$ for a limited number of parameters. We have been particularly interested in the influence on the damping and on the phase lag of the relative flatness of Ω, ie of $\hat{h}$ and of the frequency $\hat{\omega}$. We found quite soon that the discrepancy between $\hat{h}=\infty$ and $\hat{h}=1$ was surprisingly small. The least discrepancy is of course expected at the symmetry point, ie at the origin. That is demonstrated in Fig 8.

As expected, the damping and the phase increase with increasing frequency. A general conclusion is that the flatness $\hat{h}$ affects the damping more than it affects the phase lag. We also see that for $\hat{h}<\infty$ the influence of the outer region on the inner region is greater than vice versa.

Discussion

The computations presented above allow us to draw some conclusions concerning the temperature variations in the

rock around the hot water storage. The following parameters will be considered:

$T_0 = 25$ K

$a = 18$ m

$b = 38$ m

$h = 30$ m

$\kappa = 1.6 \times 10^{-6}$ m^2 s^{-1}

$\omega = 2 \times 10^{-7}$ rad s^{-1}

The average temperature of the water in the store over a complete year is 60°C. These data yield:

$\hat{b} = 2.11$

$\hat{h} = 1.67$

$\hat{\omega} = k^2 = 40.5$

Even for seasonal variations of temperature, the dimensionless frequency is high which implies that the damping is great everywhere in the rock except in the immediate vicinity of the surface of the cavern. This is extremely important since great temperature variations expose the rock to fluctuating stresses that might cause fatigue. The rock in the vicinity of the cavern is less sensitive to load since it is extensively cracked by the blasting that took place during the excavation. It is well known that all rock caverns and tunnels blasted in sound rock are surrounded by a cracked, plastic zone about 1–2 m thick. We thus conclude that no great thermally induced fluctuating stresses in the rock will occur.

We also conclude that the rock pillar in the centre of the storage carries pressure load since it has an average temperature equal to that of the water and since the damping of the temperature variations in the pillar is less than that outside the cavern.

We can calculate easily a lower limit of the damping by simple analysis for radial flow. Also, we can calculate very accurately the phase lag by radial flow. The reason for this is that in a practical case the range of variation of $\hat{b}$ and $\hat{h}$ does not differ from the values calculated above.

Finally the curves in Fig 9 indicate that the heat flux from the water to the surrounding rock compared to the corresponding heat flux to the pillar is almost exclusively determined by the parameter $\hat{b}$. In this case we see that the heat that flows between the water and the surrounding rock is approximately 4.5 times greater than between the water and the pillar. This conclusion is altered neither by the fact that the heat flow is three-dimensional nor by the fact that the heat flux from the cavern prevents T_0 from being sustained.

Acknowledgement

The authors want to thank the construction company Skanska for the permission to use the artists impression of the store shown in Fig 1.

References

1. **Carslaw H. S. and Jaeger J. C.** Conduction of heat in solids, *Oxford 1959*

2. **Brander O. and Rehbinder G.** A theoretical analysis of the dynamics of hot water underground storages. *J. Phys. D: Appl. Phys.* **16** *(1983), pp 2039–2060*

3. **Abramowitz M. and Stegun I.** Handbook of mathematical functions, *New York, 1965*

4. **Reichel L.** On the determination of collocation points for some problems for the Laplace operator, *Report Trita-NA-8006, Dept. of Numer. Anal. and Comp. Sci., Royal Inst. of Technology, Stockholm, Sweden, 1980*

5. **Reichel L.** Solving a model interface problem for the Laplace operator by the boundary collocation method. *Report TRITA-NA-8116, Dept. of Numer. Anal. and Comp. Sci., Royal Inst. of Techn., Stockholm, Sweden, 1981*

Appendix. Formulae for particular solutions

We will give explicit formulae for the particular solutions of Eq (13). We introduce:

$$f(\bar{r}') = \frac{e^{ik|\bar{r}-\bar{r}'|}}{|\bar{r}-\bar{r}'|}$$

$$g(\bar{r}') = \left(ik - \frac{1}{|\bar{r}-\bar{r}'|}\right)\frac{\partial}{\partial \xi'}(|\bar{r}-\bar{r}'|)$$

$$\frac{\partial^l f(\bar{r}')}{\partial \xi'^l} = \sum_{k=0}^{l-1}\left(\frac{l-1}{k}\right)\frac{\partial^k g}{\partial \xi'^k}\frac{\partial^{l-k-1} f}{\partial \xi'^{l-k-1}}$$

We need to compute the derivatives of g. These computations are simplified by introducing:

$$s(\xi') = \frac{1}{|\bar{r}-\bar{r}'|}$$

and

$$v(\xi') = \xi' - \xi\cos(\theta - \theta')$$

Then:

$$\left.\begin{aligned}\frac{ds}{d\xi'} &= -vs^3 \\ \frac{dv}{d\xi'} &= 1\end{aligned}\right\} \qquad \text{(A1)}$$

and:

$$g(\bar{r}') = ikvs - vs^2 \qquad \text{(A2)}$$

The formulae (A1) and (A2) lend themselves to computer-aided formula manipulation. Some of the derivatives obtained this way are:

$$\frac{\partial}{\partial \xi'}(vs) = s(-v^2s^2 + 1)$$

$$\frac{\partial^2}{\partial \xi'^2}(vs) = 3s^2v(s^2v^2 - 1)$$

$$\frac{\partial^3}{\partial \xi'^3}(vs) = 3s^3(-5s^4v^4 + 6s^2v^2 - 1)$$

$$\vdots$$

$$\frac{\partial}{\partial \xi'}(vs^2) = s^2(-2s^2v^2 + 1)$$

$$\frac{\partial^2}{\partial \xi'^2}(vs^2) = 2s^4v(4sv^2 - 3)$$

$$\vdots$$